CVPR
#8

CVPR 2020 Submission 8. CONFIDENTIAL REVIEW COPY. DO NOT DISTRIBUTE.

CVPR
#8

Accurate and Robust Trypan Blue-Based Cell Viability Measurement Using Neural Networks

Adele Peskin[1], Joe Chalfoun[2], Steven P. Lund[2], Chenyi Ling[2], Laura Pierce[2], Sumona Sarkar[2], Firdavs Kurbanov[2], Michael Halter[2], John Elliott[2]

NIST

[1]325 Broadway, Boulder, CO; [2]100 Bureau Dr, Gaithersburg, MD

adelepeskin@nist.gov, steven.lund@nist.gov, joe.chalfoun@nist.gov

Abstract

Trypan blue dye exclusion-based cell viability measurements are highly dependent on image quality and consistency. In order to enable reproducible measurements, reliable image capture with a consistent focal plane with respect to cell features and appropriate signal-to-noise ratio is required to support proper execution of image analysis routines. Current software uses human-selected features to characterize cells as dead or alive. Using neural networks to determine whether cells in a bright field image are dead or alive does not limit the range of features used to characterize these images and has removed the need to locate the sharpest image in each new sample to take a high-quality measurement. Our viability measurements can be made over a wide range of focal planes (up to 150 µm), and viability levels (0 to 100 % viability in test sets), while keeping the viability estimates within the range of manual identification of cells by several experts.

1. Introduction

Cell viability is a fundamental measurement in biological science and is used to monitor the health and quality of cells. In new medical therapies where living cells are administered to patients as the therapeutic agent, it is especially critical to carefully characterize the number of live and dead cells in the final product [1,2]. Trypan blue dye exclusion viability measurements represent a common type of imaging-based viability measurement often made using instrumentation that includes an automated microscope, proprietary imaging chambers, and proprietary algorithms designed to capture particular image features, e.g., the bright centers of live cells and dark centers of dead (i.e. membrane permeable) cells following trypan blue treatment [3,4,5]. This type of measurement has been used for many decades [6]. Live cells possess intact membranes that do not allow many substances in their environment, such as dyes like trypan blue, to pass into the cell. Dead cells do not maintain impermeable membranes and will take up the trypan blue stain, giving the cells a dark blue appearance when they are imaged [7,8].

The viability software is designed to detect the presence or absence of the blue trypan dye within the cell. Input images must be used on high contrast, sharply focused images. Under these imaging conditions live cells exhibit bright center regions and dead cells appear dark. Figure 1 demonstrates the narrow range of focal planes that can sometimes be required with commercial cell viability software to accurately represent the viability of a cell sample. The software is specific to the instrument being used; each type of instrument will have its own proprietary set of algorithms.

Using a neural network approach to measuring viability opens the door to more generalized software. If live cells have image features that differ from dead cells in the presence of trypan blue, we assumed that some of these features are robust to significant variation in focal plane. By training a network using images from a wide range of focal planes, it is possible to train a network that would discover such robust features, eliminating the need for time-consuming and variable focal plane selection. The key to finding such features is to provide the network sufficient training data to allow it to find them.

All of our image sets contain microsphere beads to indicate unambiguous high quality reference focal planes [9]. In bright field images, objects appear darker or brighter with changing focus, interfering with the ability to consistently identify live/dead cells by their brightness/ darkness. A reference focal plane defined by a consistent material such as a bead circumvents this problem. Finding the highest quality in-focus microscopic image for each cell sample is tedious and can lead to analysis errors. We use the beads here to define a high quality focal plane and assure that our neural networks find accurate viabilities both above and below this high quality plane. With appropriately trained and tested neural network models, the beads are less critical to the workflow since the models can accurately predict cell viability over a wide focal range.

CVPR
#8

CVPR 2020 Submission 8. CONFIDENTIAL REVIEW COPY. DO NOT DISTRIBUTE.

CVPR
#8
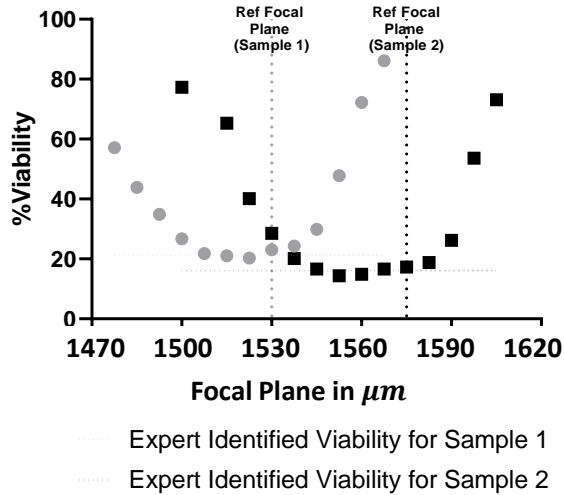
Figure 1: Percent viability analyzed by the Cellometer A2K across a range of focal planes for two samples analyzed on different days. Vertical dotted lines indicate the reference focal plane for each sample based on previously validated bead image features. Horizontal dotted lines indicate the expert evaluated % viability for each sample, where the expert manually counted cells in the images acquired by the A2K at the reference focal plane.

In this paper we outline an example of how neural network modeling can be used to accurately capture the image features of live and dead cells over a wide focal range. We show how training data was created to mimic expert manual annotation of images and compare our resulting training data with the manual annotations. We also compare the accuracy of U-Net detection and classification models [10] with these manual annotations. We apply the trained models on additional datasets to demonstrate model generalizability on new unseen data sets across wide focal ranges. Using these models, we eliminate the need for both tedious training data generation and the need for an operator to manually find the highest quality image plane in order to make a trypan blue based viability measurement.

2 Methods

2.1 Image creation

2.1.1 Sample preparation and image acquisition

We use three different datasets in this study, each with images that span a wide range of focal planes and cell viabilities (Table 1). We used five images from the first dataset for manual labeling of live and dead cells, and the rest for testing our models. We used the second data set to create training data for our neural networks. The third set was used for estimating the generalizability of the model on held out data. All our image sets contain beads to guide us to high quality reference focal planes [9]. The Bangs 100 %

ViaCheck viability control beads (Bangs Labs, VC50B, stored at 4 °C) were used to benchmark image focus.[1]

Jurkat cells (Jurkat, Clone E6-1, ATCC TIB-152) were cultured in HyClone RPMI 1640 media (HyClone # SH30096.01) supplemented with 10 % Fetal Bovine Serum (ATCC # 30-2020) and Glutamax (Thermo Fisher # 35050061) Cells were maintained in suspension culture in T-75 flasks (Corning # 1012611) at 37 °C and 5 % CO_2 and used between passage 16 and 30. Cells were prepared at concentrations of approximately 2×10^6 cells/mL for stock cell solutions.

Non-viable cells were generated via heat shock treatment. Jurkat cells were heated in 1.5 mL Eppendorf tubes (Thermo Fisher Catalog No. 3451) on a heat block (Fisher Scientific Isotemp with four blocks, Cat. No. 88-860-022) at 70 °C for a period of 30 min, followed by a 30 min recovery period in a water bath held at ambient room temperature (approximately 23 °C). The 60 % viable Jurkat cell samples, for example, are then prepared by mixing 40 µL of non-viable cells with 60 µL of healthy cells.

An aliquot of beads (between 200 and 500 µL) is centrifuged for 2 min at 6000 rcf (relative centrifugal force) and washed a total of three times with a buffer solution of phosphate-buffered saline (PBS) (Gibco Cat. No. 14040-133). Beads are then re-suspended in PBS at the original volume (200 to 500 µL). Eight (8) µL of the final bead solution is spiked into a total of 100 µL cell media for each sample. As a result, the final bead concentration used for analysis is approximately 80 000 per mL.

2.2.2 Sample preparation for Cell Count and Cell Viability Analysis

Samples were diluted 1:2 in a preparation of trypan blue (Gibco Cat. No. 15-250-061), PBS, and pre-washed Bangs 100 % viability beads to achieve a final trypan blue concentration of 0.1 %. In an optimized formulation, for every 100 µL of final suspension, 50 µL of cell suspension, 8 µL of beads, 17 µL of phosphate-buffered saline (PBS) and 25 µL of trypan blue dye are combined resulting in a 1:4 dilution of final cell suspension with trypan blue.

2.2.3 Loading samples

Bead and cell imaging studies were conducted using the Cellometer Auto 2000 (A2K) with the SD100 slides from Nexcelom Bioscience. Twenty (20) µL of the sample solution is pipetted gently into the inlet port on each chamber of the SD100 slide. The SD100 slide was then

---

[1] The mention of commercial products does not imply endorsement by the authors' institutions, nor does it imply that they are the best available for the purpose.

CVPR
#8

CVPR 2020 Submission 8. CONFIDENTIAL REVIEW COPY. DO NOT DISTRIBUTE.

CVPR
#8

inserted into the imaging chamber of the A2K. The sample was allowed to settle for at least 30 sec prior to the start of each imaging set.

Table 1: Datasets used in this study: for each set we give the focal range of the images used in μm, the reference (highest quality) focal plane in the set determined using beads, the range of viabilities in the set, and how we used each set. For set 2, each viability level had a different reference focal plane, because each new sample required refocusing.

Set	Focal range, μm	Reference focal plane, μm	Viability range %	Use
1	1470 to 1597.5, by 7.5	V0:1522 V20: 1522 V40:1552 V60:1537 V80:1515	0,20,40, 60,80	Manual labeling, model testing
2	1380 to 1612.5, by 7.5	1485	60	Training data creation
3	1477.5 to 1635, by 7.5	1053	0,20,40, 60,70, 80,100	Model testing

2.2 Manual reference viability labels

Three independent sets of measurements were made by manually labeling cells as dead or alive in images taken at the appropriate focal plane and exposure level used for the automated viability measurement, which is determined using bead features. A sample image is shown in Figure 2. The five samples of Jurkat cells were prepared at 0 %, 20 %, 40 %, 60 % and 80 % viability levels. These five images acquired on the A2K were then used as the test images for both our training data and the output of each neural network model. The manual viability measurement is determined as follows:

$$Viability = \frac{\# \ live \ cells}{\# \ live \ cells \ + \ \# \ dead \ cells} \times 100\%$$
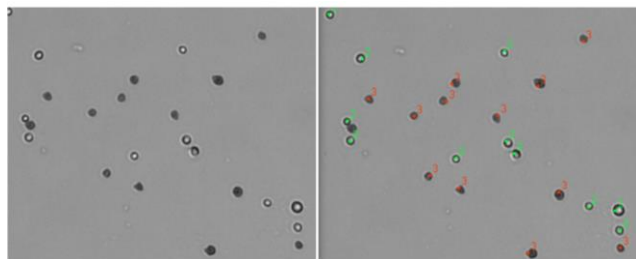
Figure 2: Example of manually labeled image: Left: section of an image; Right: section of the corresponding labeled image: 2=live cell, 3=dead cell.

2.3 Creating training data for neural networks

Additional data was needed to train the neural networks other than the manually labeled images, and so we acquired an additional set of training data using a semi-automated method. By visualizing the live and dead cells in images both in and out of focus, we saw that although the level of brightness in the center of the live cells drops with image focus, the center of the live cells look different from their cell edges at all focus levels. Figure 3 shows example live and dead cell images across the focal range of this experiment. The centers of the dead cells do not exhibit as large a pixel intensity range as the centers of the live cells at all focal levels. We use this difference between the live and dead cells to label them automatically. We collected cell centers at a wide range of focal levels and separated the live from the dead cells based on cell center pixel uniformity. In order to do this, we first segmented and separated all cells in each image as explained in the next section.

We used a set of 39 bright field images from Dataset 2, covering a range of focal values of 135 μm, from 60 μm below the reference plane to 75 μm above the reference plane. These samples were all prepared at approximately 60 % viability. The 135 μm range covers most of the images for which the live and dead trypan blue stained cells have morphological differences. The brightest live cell centers appear at the reference focal plane, although planes above and below the reference focal plane also have bright centers. This is reflected in the viability measurements in Figure 1, which remain stable over a small focal range for both samples in that experiment (approximately 22.5 μm for sample 1 and 30 μm for sample 2).

CVPR
#8

CVPR 2020 Submission 8. CONFIDENTIAL REVIEW COPY. DO NOT DISTRIBUTE.

CVPR
#8
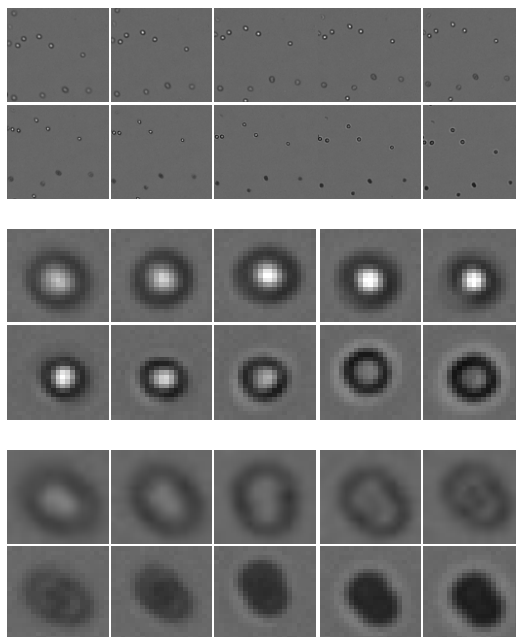
Figure 3: Live and dead cell images across the focal range of this experiment. Top: closeup of a region of each image showing live and dead cells; Middle: closeup of the same live cell from each image; Bottom: closeup of the same dead cell from each image. For each set of pictures: Top row of each: image sample at 1425,1440,1455,1470,1485 µm; Bottom row: image sample at 1500,1515,1530,1545,1560 µm. The sample at 1485 µm has the highest quality focus.

2.3.1 Cell separation

In order to collect image pixels from the centers of each cell, it was necessary to first separate the cells in the image from one another. We do this using a software pipeline that includes finding cell edges using the Empirical Gradient Threshold (EGT) method [11], followed by cell separation using the Fogbank segmentation method [12]. The parameters for each of these methods are outlined in Table 2. Parameters for the Fogbank segmentation often need to be tuned with each image, thus limiting the number of images in our training set by this labor intensive process. An example image is shown in Figure 4, along with its resulting cell-separated mask. We use the outcome of our neural network to generalize the painstaking task of cell separation.
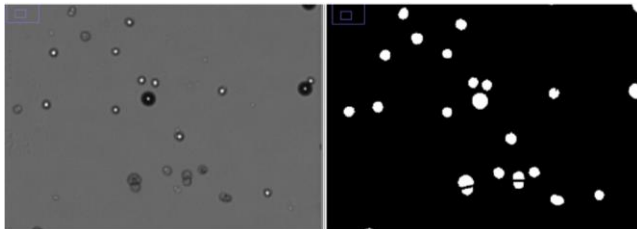
Figure 4: Example of cell separation by EGT and Fogbank: on the left is a section of an image taken at the reference focal plane, 990. On the right is the corresponding mask of separated cells.

Table 2: Parameter for cell separation

EGT parameters	FogBank parameters
Min_cell_size:[50 to 80]	Min_peak_size: [10 to 30]
Min/max hole_size: Inf	Min_object_size:[50 to70]
Hole_min_percent_intensity: [70 to 95]	Fogbank_direction: 2
Hole_max_percent_intensity: 100	Percent_binning: [5 to 20]
Fill_holes_bool_oper: 2	
Manual_finetune: [-15 to 2]	

2.3.2 Automated cell labeling by cell center pixel intensities

Once the cells are cleanly separated, the center set of pixels are collected and averaged. We use the centroid of each pixel cluster as our center location. Two different sets of center cell pixels are collected, a 3x3 pixel set, and an 8x8 pixel set, because at different focus levels, the center cell pixel diversity covers a different size range. The mean and standard deviation of each of these sets is found and the standard deviations are sorted smallest to largest for each image. The ratio of the mean pixel intensity at a 3x3 center to the mean intensity of the whole cell indicates whether to use a 3x3 or an 8x8 center. The most in-focus live cells have very bright centers that fill the 3x3 center. Out of focus cells centers cover a wider portion of the cell, and for those we sort and use 8x8 pixel centers. We used a ratio of 2:1 (center 3x3 pixels to whole cell) to determine which size to use. For cell centers with a ratio greater than 2, we use the 3x3 center pixels. The cutoff between live and dead cells is determined by the largest change of slope of the sorted list of standard deviations and we tested this cutoff by a comparison with the manually labeled cells.

2.4 Semantic segmentation networks

Six different models were trained using images with different sets of focal ranges from Dataset 2. Table 3 lists those ranges. In order to compare viability results across different data sets, each with its own reference focal plane, we describe each model in terms of its Z range above and below the reference focal plane corresponding with each image. We ran a U-Net [10] network using images from the prescribed set of focal planes, and labeled masks prepared as described above with four class labels: background (0), beads (1), live cells (2), and dead cells (3). Batch sizes of 12 were fed into the network, with initial learning rate = 3.0e-4, adjusted by an Adam optimizer. All images were zscore normalized as whole images, then tiled into 256x256 tiles to go into the network. We found that a tile-by-tile normalization led to less accurate network outcomes.

Table 3: Focal ranges used for training the segmentation models

model	Z Range , µm	Range µm (0 µm is at reference focal plane, 1485)
1	1425 to 1560	-60 to 75
2	1470 to 1560	-15 to 75
3	1470 to 1545	-15 to 60
4	1470 to 1530	-15 to 45
5	1455 to 1530	-30 to 45
6	1440 to 1530	-45 to 45

CVPR
#8

CVPR 2020 Submission 8. CONFIDENTIAL REVIEW COPY. DO NOT DISTRIBUTE.

CVPR
#8

2.5 Semantic segmentation network output viability calculation

Six different models were trained using images with different sets of focal ranges from Dataset 2. A viability was determined from the output of each of the six network models. Since the classification from the network is done pixel by pixel, the type of cell represented by each pixel cluster is determined by the class with greatest presence. The viability was then determined by the number (live cells)/(live + dead cells). Cells that are touching, resulting in larger pixel clusters, are treated as multiple cells depending upon the size of the pixel cluster. After inferencing each of the six models on the five images used for manual labeling, each cell was then compared with one of the cells that had been manually labeled for a cell to cell comparison.

3 Results

3.1 Manual label results

The three sets of labeled live and dead cells were compared with one another to determine the level of accuracy expected from model outcomes. Overall viability measurements from each expert are shown in Table 4. We include average measurements across the three experts to show the variability from expert to expert.

Table 4: Manually labeled viability counts from three experts and the variability among them as shown by the standard deviation (stddev) of measurements at each viability level. All numbers given in percent viability.

Viability level	Expert 1	Expert 2	Expert 3	Mean	Stddev
0 %	2.59	3.08	3.04	2.90	0.22
20 %	17.90	18.36	18.75	18.34	0.35
40 %	30.00	32.58	31.97	31.52	1.10
60 %	53.91	56.22	54.43	54.85	0.99
80 %	74.13	79.50	76.92	76.85	2.19

We used the manually labeled images also to assess the quality of our training data generation, and the quality of the output of our neural networks. To do this, we used our method to create training data on the same five images that were manually labeled. We also ran our six neural network models outlined in Table 3 above with the same five images. A comparison of how close the training data and network output data is to the manual labels is shown pictorially in Figure 5 below. The dendrogram was made using the R [13] hclust function for hierarchical clustering with default settings. One set of the expert labels is closer to the training data than to any other set of measurements, including the other two expert labels. The same set of expert labels is closer to three of the model outputs than to

the other two expert labels. The viabilities from the six network models on the test five images are shown in Table 5. Models 4,5, and 6 (Table 3) were closer to the manual labels than those using higher focal planes.
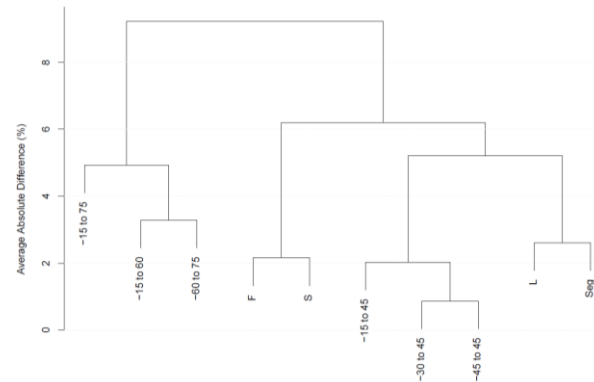
Figure 5: Cluster dendrogram with branches demonstrating which viability measurements were closest to one another. The expert measurements are labeled as F,S,L, training data is labeled as Seg, and the model outcomes are labeled by their focal ranges. One of the expert labels (L) is closer to the training data than any other set of measurements. Three of the model outcomes are closer to L than to the other expert labels.

Table 5: Network output % viability: viabilities measured on masks output from the neural net models showing focal ranges of models.

V %	-60 to 75	-15 to 75	-15 to 60	-15 to 45	-30 to 45	-45 to 45
0	10.04	0.83	1.21	0.40	13.76	10.44
20	17.13	17.26	18.11	16.73	18.22	20.32
40	31.54	31.56	31.68	31.32	32.22	33.72
60	52.52	54.31	54.94	54.24	54.72	56.02
80	73.75	73.54	73.36	71.54	74.27	76.81

Disagreement between the live/dead cell individual labels is shown in Figure 5 for each of the 5 test conditions. The manual labels disagree with each other by 3 to 8 %. The training data labels are similar to one another but disagree with the manual labels by 8 to 10 %. The model output labels disagree by 10 to 15% except for the image with 0 % viability, where the disagreement was much higher. Even though individual cells were labeled differently, the overall viability numbers are very close to one another for all sets, seen in Figure 6.

CVPR
#8

CVPR 2020 Submission 8. CONFIDENTIAL REVIEW COPY. DO NOT DISTRIBUTE.

CVPR
#8
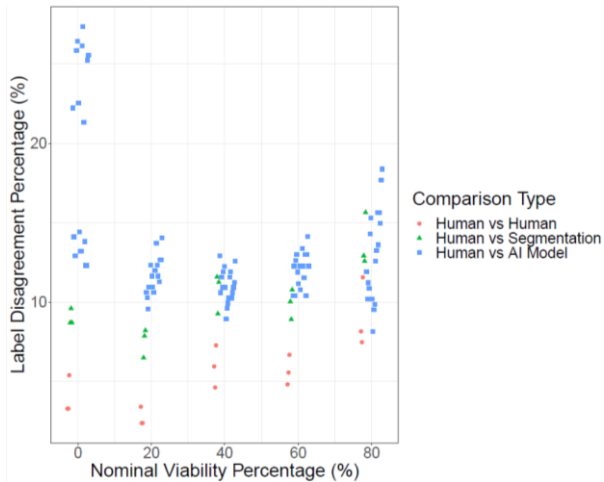
Figure 5: Plot showing how the manual labels (red) disagree with each other and with the training data labels (green) and the labels output from the models (blue).
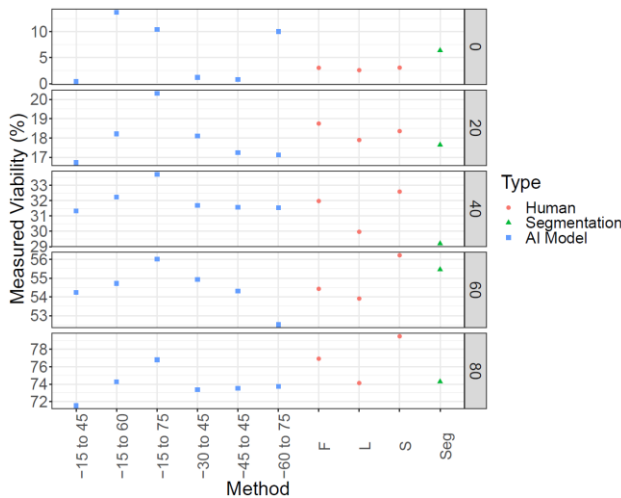
Figure 6: Chart showing overall viability measurements for the five test images, comparing manual labels (red), training data labels (green) and model output labels (blue). The six models are labeled on the x axis by their focal ranges.

3.3 Additional network viability tests

Each network model was used to inference images in two additional sets of data, each of which covered a range of viabilities and a range of focal plane values. For each set, we were interested in consistent viability measurements from a model across a wide focal range. We do not have manual labels for cells in all of these sets, but we do have an approximate viability number based on how the images were acquired. For example, a 70 % viability estimate is made for images from solutions of 70 % live, 30 % dead cells. We assume the resultant viabilities measured from these images will be close to 70 %, although each image will vary from the others. Table 6 shows resulting viability data from masks output from each of our six network

models on images from Dataset 1. Table 6 shows mean viabilities across full focal sweeps and the corresponding standard deviations to show their consistency.

Table 6: Means and standard deviations (stddev) of the output on the Dataset 1 images from the three models closest to manual labeling. Images covered a span of 127.5 μm

Model focal range	Viability estimate (%)	Model Viability mean (%)	Model Viability stddev (%)
-15 to 45	0	3.3	1.3
	20	18.9	1.2
	40	37.1	2.1
	60	58.8	2.4
	80	76.0	1.0
-30 to 45	0	6.9	2.5
	20	20.5	1.9
	40	38.0	2.5
	60	62.0	3.0
	80	76.7	1.0
-45 to 45	0	0.4	0.1
	20	14.5	0.8
	40	28.5	1.5
	60	47.5	1.8
	80	68.2	1.8

Each of the six neural network models was used to predict viability levels for all of the images in Datasets 1 and 3. Figure 7 shows the predicted viabilities on the y axis plotted against the associated Z level for each test image. In order to compare outcomes, the x axis shows Z levels in terms of a distance from each reference focal plane; i.e., the Z distance to the highest quality image, in which bead edge gradients were highest.

Our best results are seen in the output of Dataset 3, where three of the models (-15 to 45, -15 to 75, -60 to 75) predict consistent viabilities over the Z range of approximately 100 μm for each of the seven viability levels. Viabilities predicted for Dataset 1 show consistency over a 75 μm range around the reference focal plane for each experiment. However, for the higher z levels, the viabilities vary more than 5 %. At these values, it is not clear whether our models are not as accurate, or whether the cells that are being imaged are starting to die, since these images were the last ones acquired in the image sweeps. More tests are needed to distinguish between these two possibilities.

Several anomalies are also seen in the 40 % viability data. Of the four views that are imaged, the D view consistently has varied outcome because there was a large piece of

CVPR
#8

CVPR 2020 Submission 8. CONFIDENTIAL REVIEW COPY. DO NOT DISTRIBUTE.

CVPR
#8

debris on this image that our model was not able to handle. In addition, there is a consistent error in the first Z views at Z=1500, where we suspect the dead cells did not have sufficient time to take in the trypan blue and still appeared to have bright centers. Future work with a larger training set that covers a wider Z range will help to answer these questions. It is possible that with model improvements, that we will be able to find images in which cells start to die over time by using a viability neural net model.
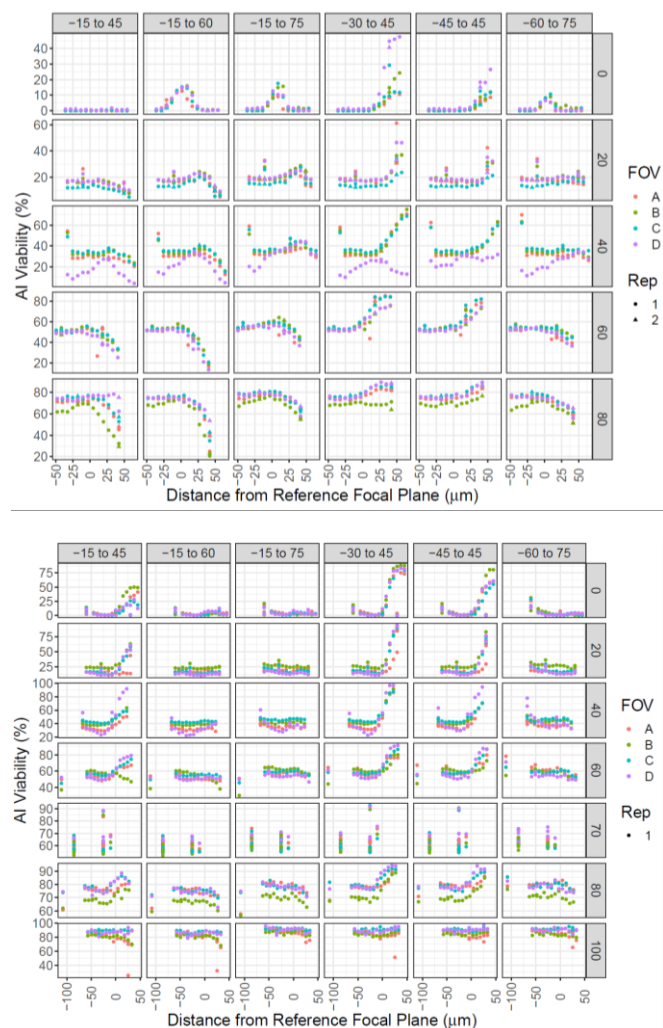
Figure 7: Outcomes from the six neural network models at all viability levels (labeled at right in gray) and across all Z levels available in the data, labeled along the x axis by the distance from the reference focal plane (highest quality image plane) of each individual sample for comparison. Top: Dataset 1, Bottom: Dataset 2. For each Z and viability combinations, the microscope takes four fields of view (FOV), and for most combinations there are replicate sets (Rep. labeled in the figure).

4 Conclusions

Conventional microscopy software algorithms for viability measurements depend upon specific cell image features to correctly label cells as alive or dead. In our examples, we showed viability data in which the built-in instrument trypan blue viability analyzer software gave consistent viability measurements over approximately 25 µm ranges. Image features (in particular the brightness of cell centers) change at different focal planes, making the usefulness of the viability algorithms dependent on returning to specific high-quality focal planes. These high-quality planes can in turn be difficult to identify consistently. We have used a neural network approach to make these measurements less dependent upon focusing the microscope correctly, resulting in viability measurements that are reasonable across a wider focal range (75 to 100 µm over all viability levels), with an accuracy that mimics that of manual labeling.

In a series of different steps, we have shown that we can generate a limited amount of training data for a U-Net cell classifier that is as close to manual labeling as several experts are to one another. From this training data, made at a single viability level with images spanning 75 to 100 µm focal ranges, we have generated classification models whose output viability measurements are also similar to those from the manually labeled images. In the process, we eliminate future need for manual cell labeling and generating semi-automated cell and dead cell training data. We can use our neural network models on a wide range of focal planes, eliminating the need to get an accurate auto-focus of the cells in an image in order to acquire an accurate viability measurement.

References

[1] S. Lin-Gibson, S. Sarkar, Y. Ito. Defining quality attributes to enable measurement assurance for cell therapy products. Cytotherapy. 2016 Oct 1;18(10):1241-4.

[2] S.R. Bauer. Stem Cell-based Products in Medicine: FDA Regulatory Considerations. Handbook of Stem Cells. 2004:805.

[3] [7] J. Tennant, Evaluation of the trypan blue technique for determination of cell viability, Transplantation, 2,6,685-694, Nov. 1964.

[4] C.M. Garvey, T.A Gerhart and S.M Mumenthaler, Discrimination and Characterization of Heterocellulr Populations Usng Quantitative Imaging Techniques, *J. Vis. Exp.,* vol. 124, 2017.

[5] S. Busschots, S. O'Toole, J.J. O'Leary, B. Stordal, Non-invasive and non-destructive measurements of confluence in cultured adherent cell lines, https://doi.org/10.1016/j.mex.2014.11.002, Nov 2014.

[6] S.M. Hammoudeh, A.M Hammoudeh, R. Hamoudi, High-throughput quantification of the effect of DMSO on the viability of lung and breast cancer cells using an easy-to-use

CVPR
#8

CVPR 2020 Submission 8. CONFIDENTIAL REVIEW COPY. DO NOT DISTRIBUTE.

CVPR
#8

spectrophotometric trypan blue assay, Histochemistry and Cell Biology, 152:75-84, 2019.

[7]   W. Strober, Current Protocols. 21(1) A.3B.1-A.3B.2, May 2001.

[8]   K.S.Louis, A.C> Siegel, Cell Viability Analysis using trypan blue: manual and automated methods, Mammalian Cell Viability, Methods in Molecular Biology (MIMB). 740, pp.7-12, March 2011.

[9]   A. Peskin, S. Lund, L. Pierce, F. Kurbanov, L. Chan, M. Halter, J. Elliott, S. Sarkar, J. Chalfoun, Establishing a Reference Focal Plane Using Beads for Trypan-blue-based Viability Measurements, J. Microscopy, accepted.

[10] O. Ronneberger, P. Fischer, T. Brox. U-Net: Convolutional networks for biomedical image segmentation. Medical Image Computing and Computer-Assisted Intervention (MICCAI), 234-241, 2015.

[11] J. Chalfoun, M. Majurski, A. Peskin, C. Breen, P. Bajcsy, M. Brady, Empirical gradient threshold technique for automated segmentation across image modalities and cell lines, J. Microscopy, 260(1):86-99, 2015.

[12] J. Chalfoun, M. Majurski, A. Dima, C. Stuelten, A. Peskin, M. Brady, FogBank: a single cell segmentation across multiple cell lines and image modalities. BMC Bioinformatics, 15:431-442, 2014.

[13] R Core Team (2020). R: A language and environment for statistical computing. R Foundation for Statistical Computing, Vienna, Austria, https://www.R-project.org/.